

SCHOOL OF PHYSICS AND ASTRONOMY

ASTRO Y2 LABARATORY

Second Semester Report

2019

Determining the weather on an Exoplanet

Astle Fernandez, Sharif Khan-Bennett, Alice Purdy

Tutor: Dr. Carl Wheldon

Abstract:

We present a complete and partial analysis of the lightcurves of Kepler-2 and Kepler-7 systems respectively, with an aim to obtain the physical parameters defining these systems (primarily the albedo and temperature) along with a thorough error analysis. We calculated a value of $2133.91 \pm 103.84\text{K}$ and 0.14 ± 0.07 for the temperature and albedo of the planet Kepler-2b respectively, which agrees with previously attained values. Using this data, we suggest a possible composition in its atmosphere. We also present two models for the primary transit and one for the secondary transit, the best fit to the data and suggestions for improvement.

Introduction:

This project relies on the principles of transit photometry, a process in which the flux from a star is monitored for a significant period and analysing the various properties of the resulting lightcurve to determine various properties of the stellar system. The lightcurves we obtained were from the NASA MAST website^[1], which presents the data in short and long cadence intervals. This data was collected by the Kepler telescope, which helped detect over 2300 exoplanets^[2], with unprecedented precision.

The presence of an exoplanet would produce dips in the lightcurve, enabling us to determine its size, period and other physical properties. The exoplanet chosen was Kepler-2b(or HAT-P 7b)^[3], owing to its significant size, low albedo and a relatively short orbital radius which will be discussed in the following section.

Theory:

As an exoplanet transits between the star and the observer, some the host star's light is blocked which can be observed in the lightcurve (provided its orbital plane lies parallel to our line of sight) and is termed the primary dip. This dip is proportional to the ratio of the areas and hence we can determine the relative planet radius R_p from the equation^[4],

$$R_p = R_s * \sqrt{1 - \Delta F}, \quad (1)$$

where R_s is stellar radius and ΔF the normalised maximum dip in intensity.

Since this dip is seen every time the planet completes an orbit, we can calculate its period and then calculate its orbital distance a from a rearrangement of Kepler's third law:

$$a = \sqrt[3]{\frac{GMP^2}{4\pi^2}}, \quad (2)$$

where G is the gravitational constant, P the period and M approximated to the host star's mass.

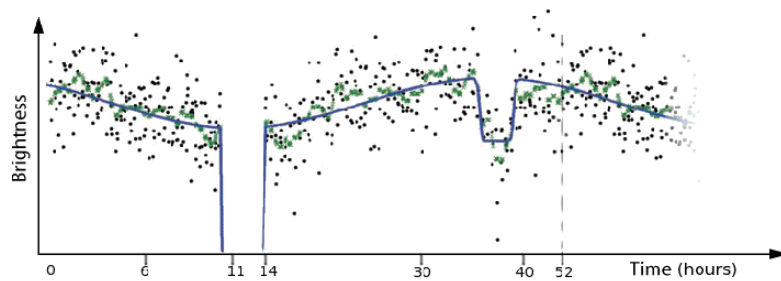


Figure 1: Sample lightcurve of Kepler 2, showing the primary dip, secondary dip and the variation of intensity between them.^[5]

However, for large exoplanets (Neptune-Jupiter sized), we can also observe a smaller dip called the secondary or ecliptic dip as the planet is occulted by the star. This is because when the planet isn't causing the primary dip, a fraction of the light incident on the planet is reflected towards us, a fraction which increases and reaches a maximum just before transiting behind the star. The intensity of this

light is proportional to the ratio of the reflected and incident (on the planet) fluxes of the exoplanet. In addition to this, we must also consider the reflectivity of the exoplanet which is termed the albedo. An albedo of 1 indicates total reflection of incident light and 0 represents complete absorption. Thus, the albedo provides a glimpse into the composition of the exoplanet's atmosphere and can be used to determine the cloud circulation. We can now calculate albedo during the ecliptic dip A_g , (called the geometric albedo) using the equation,^[5]

$$A_g = (F_p/F_s) * \left(\frac{a}{R_p}\right)^2, \quad (3)$$

where F_p and F_s are the stellar and planetary fluxes respectively.

It is important to note that this value for albedo is only accurate at that given phase (say π , phase is zero during transit midpoint and secondary transit occurs half-period later). Therefore, we use bond albedo A_b , which gives the albedo averaged over the period providing a more general value to determine the planetary temperature, for instance. The bond albedo is related to the geometric albedo from the equation,^[6]

$$A_b = qA_g, \quad (4)$$

where q is the phase integral, which can be calculated by,^[6]

$$q = 2 \int_0^\pi \left(\frac{I(\alpha)}{I(0)}\right) * \sin(\alpha) d\alpha, \quad (5)$$

where α is the orbital phase, $I(\alpha)$ the intensity incident on the planet at that phase and $I(0)$ the stellar intensity.

If we normalise the fluxes, $I(0)$ becomes 1. The phase integral encodes the fraction of light reflected towards us at a given phase and the factor of 2 to account for the whole period.

We also need the luminosity of the host star L_s to calculate the global effective temperature T_{eff} of the exoplanet which is done using a rearrangement of the standard luminosity-distance relation,

$$L_s = L_v \left(\frac{D_s}{D_v}\right) * 10^{-\frac{m}{2.5}}, \quad (6)$$

where L_v is the luminosity of Vega, m the magnitude of the host star and D_v , D_s are the distances between Vega and the host star from us respectively.

Having calculated these values, we can now determine the global effective temperature of the host star from Stefan-Boltzmann's law^[7]:

$$T_{eff} = \left[\frac{(1-A_b)L_s}{16\pi\sigma a^2}\right]^{\frac{1}{4}}, \quad (7)$$

where σ is the Stefan-Boltzmann constant.

The factor of $(1 - A_b)$ accounts for the light absorbed by the exoplanet and 16 instead of 4 due to the flux luminosity relation.

Procedure:

Obtaining the data:

Our initial task was to obtain the data for Kepler 7(Kepler ID:5780885)^{[8][9]} and Kepler 2(KID:10666592). Kepler provides data with time resolutions of ~1minute and ~30 minutes called short (SC) and long cadence (LC) respectively. We based our work on the SC data initially but later changed to LC due to lightcurve's^[10] query limitations.

Initial Plotting:

The data was present in a .FITS file format and we used the pandas module in python to extract the data from all the lightcurves into a single .csv file which would be easier to access and modify. The data was then plotted, and the result is shown in Figure 2.

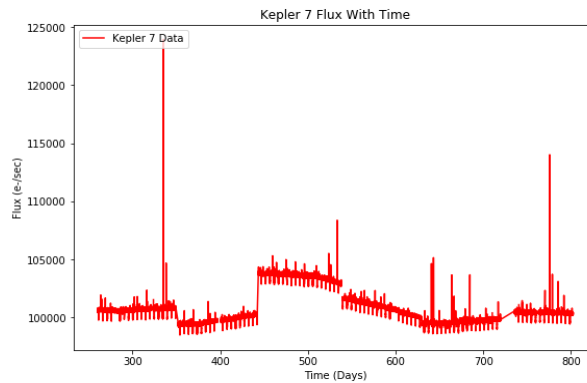
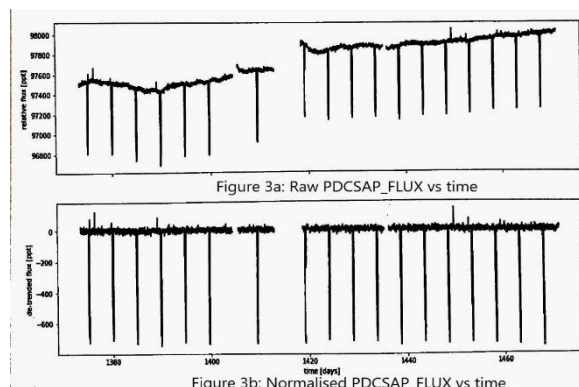


Figure 2: Kepler 7 lightcurves ('SAP_FLUX' vs time).

The data was available in two formats namely the Simple Aperture Photometry Flux ('SAP_FLUX') and Pre-search Data Conditioned SAPFLUX ('PDCSAP_FLUX').^[11] The latter has the various systemic artefacts or trends subtracted from the former, hence has some of the noise removed and we resolved to use it. These trends are individual to the detectors in the Kepler telescope and are obtained by viewing relatively quiet stars. There are 16 trends per detector and were updated every observing quarter. SAP_FLUX is the summation of flux falling in the pixels within the pre-determined aperture.^[11]

Despite the irregularities from the flux being incident on different pixels throughout the observing period as well as the points in time where no data was available, there are periodic dips in intensities which could be due to the primary transits. Due to the processing time required to simply read and plot all the lightcurves, we decided to choose a sample lightcurve and write the code to process it which could then be extended to all the lightcurves. The sample data was taken from a 2013 dataset (observing quarter 15). Using the astropy module for python, we extracted the SAP_FLUX and PDCSAP_FLUX columns and plotted them against time. The raw and normalised PDCSAP_FLUX vs time graphs are shown in *Figure 3a* and *b*.



As seen from the figures above, the normalised graph shows in much more detail the primary dips, while the secondary dips are still obscured by the noise. There were also periods when data wasn't being collected, hence missing the primary dips.

Processing the data:

Our next step was to clean the signal further. We removed the rows where Kepler wasn't recording the intensity, i.e., when the 'TIME' column had no data in it. There were also instances where the PDCSAP_FLUX and the PDCSAP_FLUX_ERR didn't have a numeric value; these were filled with median values of the observing quarter. The lightcurves were then stitched together and plotted the trend line obtained from `scipy.signal.medfilt()`.^[12] The trend line was subtracted from the intensity values, giving the normalised graph. The resulting graph was very similar to the one obtained in *Figure 2*, but without the undesired pauses in data. However, most of the primary transit dips were also smudged out in the normalised graph, and we had to find alternative methods to clean the data.

We decided to use the in-built functions from `lightcurve` to reduce the noise. Knowing the Kepler identification number, we were able to use the `search_lightcurve()` function to get lightcurves from all the observing quarters and stitch them into a single lightcurve object. `Lightcurve` also provided a host of other functions including the `remove_nans()` [to remove all the not a number (NaN) values], `flatten()` [to remove low-frequency noise and return a median trend] and `normalise()` functions to help clear out the noise.

The best fit period was obtained by using the `periodogram()` function, which applies a Fourier transform on the data and returns the strengths of the signals in the data. Periodograms of Kepler-2 and Kepler-7 are shown in figures 4a and 4b respectively.

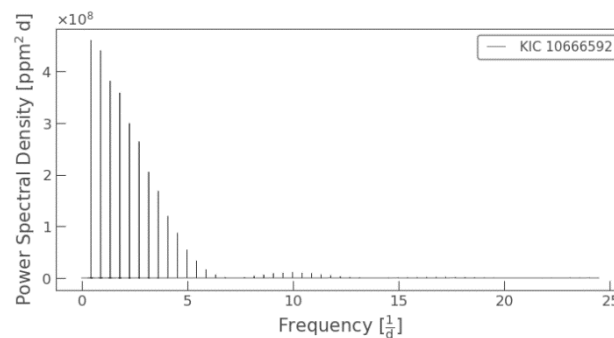


Figure 4a: Periodogram of Kepler 2.

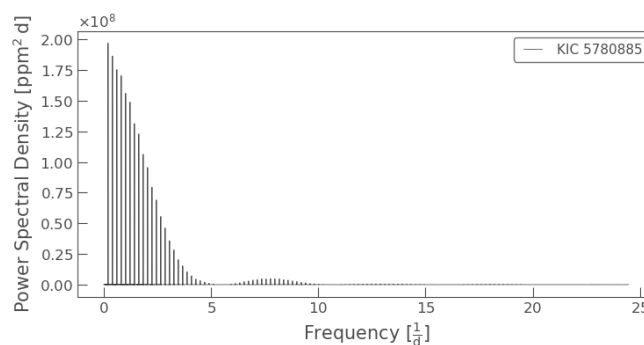


Figure 4b: Periodogram of Kepler 7.

We observe that the strongest frequency corresponds to the period of the exoplanet followed by its higher order harmonics. We also observe almost sinusoidal envelope peaking at about 10d^{-1} and 8d^{-1} in 4a and 4b respectively, which can be attributed to the oscillations in stellar intensity, arising from the seismic waves trapped in the star.^[13] The inverse of the strongest frequency is now used to calculate the period. Since we picked one frequency, the module assumed no error and hence we had no error on our period.

We phase-folded the complete lightcurves for the two systems using the periods we obtained, and the resulting plots are shown in Figures 5a and b. The size of the lightcurve files minimises the short-term random noise. The data was binned with bin-size=13.

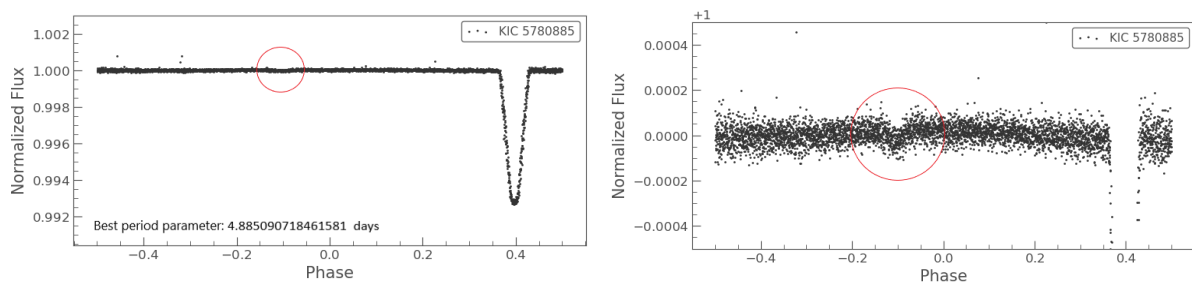


Figure 5a: Phase folded result for Kepler 7, with best period parameter and possible eclipse dip.

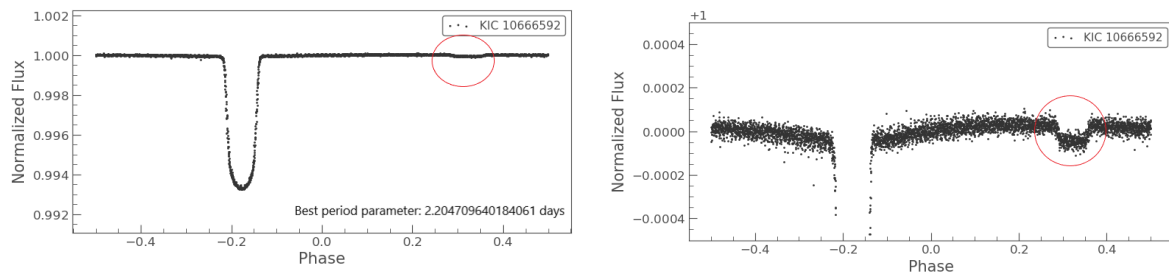


Figure 5b: Phase folded result for Kepler 2, with best period parameter and possible eclipse dip.

We realised from Figure 5a that the secondary dip caused by Kepler-7b is tiny; $<0.02\%$ dip in the star output. In fact, despite the general outline expected of an eclipse is present, we observe the noise is still of a comparable magnitude and requires more processing to get an accurate result for the fractional secondary dip. We also note that the best period parameter is ~ 4.885 days, which corresponds to an error of 0.0084% , very close but still not within the accepted error range (4.88553 ± 0.00004 days).^[9]

From Figure 5b however, the results seemed more promising; we observe a clear secondary dip as well and the variation in intensity between the primary and secondary dips, which could be attributed to lower noise. This is partially confirmed when we compare the best fit parameter (shown in Figure 5b) with the accepted value ($2.204735471 \pm 2.4\text{e-}06$ days)^[3], an error of 0.001% . It could also mean that the planet has a high emissivity and very low albedo, which will be calculated in the following section. We decided to focus our investigations solely on Kepler-2.

Obtaining the physical parameters:

- **Calculating planet radius**
Using equation (1) we can calculate the relative radius of the planet with respect to the host star after finding the primary dip. Since the phase folded data has a non-zero thickness at the minimum of the dip, we decided to calculate the mean of the dip and then added the errors of those values in quadrature. The true radius of the planet can be calculated by quoting the star radius from scientific literature, but it was easier to use the normalised values of planet radii and orbital distance to calculate the other physical properties and modelling.
- **Calculating orbital distance**
Using the period given from the periodogram and equation (3), we can determine the normalised orbital distance. We also note that the sum of the masses has been approximated to the host star's mass, as the error in ignoring the planet mass is not significant to the error in host star's mass (*detailed in the Results section*).
- **Determining the secondary dip**
It was harder to calculate the secondary dip compared to the primary, which is why the error values are almost 25% the value. The total flux has been normalised, so this dip is equal the intensity of the reflected light from the planet. Error estimation was done similar to the primary dip.
- **Finding the albedo**
Since we have already found the normalised orbital distance and planet radius, we can use equation (3) to determine the geometric albedo. Errors were propagated from the dependant quantities.
- **Calculating the bond albedo**
Finding the bond albedo required the phase integral. The lightcurves were snipped to only get the intensities between the primary and secondary transit dips. The times series was converted to the corresponding phase angle and the integration can be reduced to summation using the formula,

$$q = 2 \int_0^\pi \left(\frac{I(\alpha)}{I(0)} \right) \sin(\alpha) d\alpha \approx 2 \sum_{\alpha=0}^\pi I(\alpha) \sin(\alpha), \quad (8)$$

where α is the phase angle.

To obtain the $I(\alpha)$ values, we compute a linear best fit for the data, done with `scipy.stats.linregress()`^[12], returning the slope and intercepts with their respective errors. The resulting line and data are shown in Figure 6.

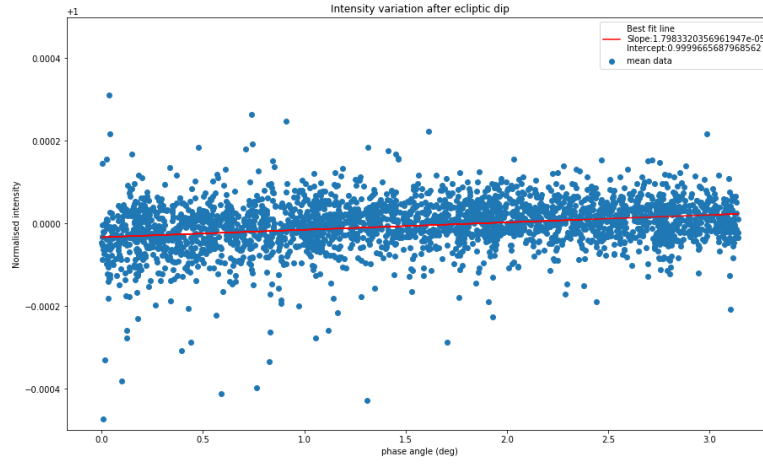


Figure 6: Intensity variation after an ecliptic dip with best linear fit for Kepler 2.

Error in the phase integral was obtained from the errors in intensity and then propagated to the bond albedo.

- **Effective global temperature**
We calculated the global effective temperature, which was compared to values in scientific literature (*see Results*). Standard error formulae were used.
- **The impact parameter and inclination angle**
Another important physical parameter which affects the transit dip is the inclination of the orbit (i), calculated from the impact parameter (b).

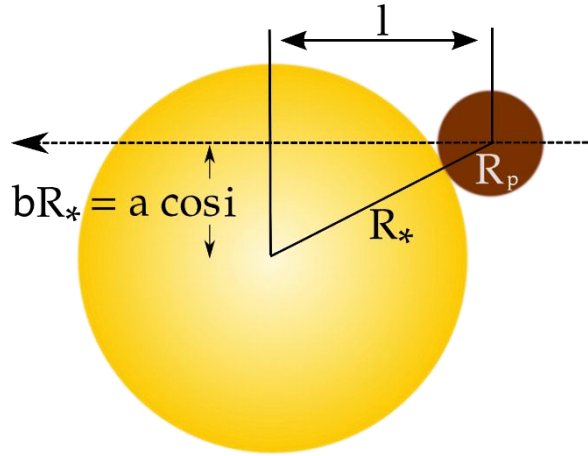


Figure 7: Transit path geometry where transit length l is given by:

$$l = \sqrt{(R_s + R_p)^2 - (bR_s)^2}. \quad (9)^{[4]}$$

An exoplanet with an inclined orbit will spend a shorter time in transit, leading to a more a sharper dip and shallower dip. The shallowness is because of limb-darkening, i.e. when the fringes of a star appear (to the observer) to contribute less to the overall brightness compared to the centre. This means that a planet orbiting with some inclination will block light from the fainter areas of the star, leading to smaller dip in intensity.

Approximating the planet to travel a straight path, we can use the transit duration t from the light curve to determine the impact parameter of the planet using the relation,^[4]

$$t = \frac{P\alpha}{2\pi} = \left(\frac{P}{\pi}\right) \sin^{-1} \frac{l}{a}, \quad (10)$$

where α is the angle swept by the exoplanet while travelling the length $2l$, i.e. the period between entering and leaving transit. Inclination angle is calculated from,

$$i = \cos^{-1}((R_s b)/a). \quad (11)$$

Again, standard error propagation was done to find the errors.

It should be noted that we chose to model the transit curve assuming the star to be a uniform sphere, which may lead to some error in the values obtained.

Modelling:

Although we could calculate most of the physical parameters from Kepler 2's lightcurve by visual inspection and constraints, we realised that we needed to develop a model to extract these parameters, since we wanted to replicate the process for smaller planets (Candidate: Kepler-78b^[14]) which will show fainter dips. These planets were chosen due to their high reflectivity, short periods, high a/R_s ratio and part of a single-planet system.

The first primary transit model used was the uniform source model [Mandel and Agol, 2002] in which the obscured flux F is given by the function:^[15]

$$1 - F = \begin{cases} \left(\frac{1}{\pi}\right) * [\kappa_0 p^2 + \kappa_1 - \sqrt{0.25 * (4z^2 - (1 + z^2 - p^2)^2)}], & |1 - p| < z \leq 1 + p \\ p^2, & z \leq 1 - p \\ 1, & z \leq p - 1 \\ 0, & \text{otherwise} \end{cases} \quad (12)$$

κ_0, κ_1 are given by

$$\kappa_1 = \cos^{-1}[(1 - p^2 + z^2)/2z] \text{ and} \quad (13)$$

$$\kappa_0 = \cos^{-1}[(p^2 + z^2 - 1)/2pz] \quad (14)$$

where z and p are the normalised orbital and planetary radius.

A model was made for Kepler-2 using the above relations, but due to computation time later abandoned.

We later designed a 3-parameter (planet radius, star radius and stellar intensity) model using principles of convolution to get the expected lightcurve. This was done by creating two semi-circles with the planet and star radii. Assuming an inclination of zero for the planet orbit, the semicircle corresponding to the planet was moved along the x-axis and the area of overlap between these semi-circles were calculated at each step and the intensity expected was calculated. It should be noted here that the orbital distance was not a parameter in the model because it was set manually outside the function. The model was fitted to the Kepler data and results noted.

A slightly more complex 4-parameter model (3 + impact parameter) was also constructed to achieve a better fit. As stated earlier, we assumed a uniform source for the host star hence we obtain the same dips in intensity for the given 3 parameters and varying the impact parameter changes the transit duration.

Finally, a simple secondary transit model was also coded, as this would help in the extraction of the secondary dips and mandatory for the smaller planets with the fainter dips. This model didn't perform as well as expected when fitted to Kepler-2 data, and the possible shortcomings are explained.

Results:

Physical parameters:

- Period obtained from the periodogram was 2.204737 days, which agrees with approved value ($2.204735471 \pm 2.4e-06$). We couldn't get an error range for our period as mentioned before.
- The mean of the primary dips for Kepler-2 was found to be 0.99325 ± 0.00003 . Mean error was calculated from:

$$\delta F = F * \sqrt{(\sum_i^n \delta x_i^2)/n}, \quad (15)$$

where n is the number of points at minimum of the dip.

The relative planet radius was determined to be 0.0821 ± 0.0145 (stellar units). This indeed falls with the error range of the accepted values and a complete list of the physical parameters obtained with those found in scientific literature are shown in *Table 1*.

With R_s of $1.84 \pm 0.23 R_\odot$ ^[3] the planet radius was determined to be $1.05 \pm 0.13 * 10^8$ m.

- The normalised orbital distance was found to be 4.407 ± 1.49 (stellar units) or $5.64 \pm 1.02 * 10^9$ m which also agrees with previously determined values. Error in the orbital distance was determined from the relation

$$\delta a = a * \sqrt{\left(\frac{1}{3}\right) * \left[\left(\frac{\delta M}{M}\right)^2 + \left(\frac{\delta G}{G}\right)^2\right]}, \quad (16)$$

where M, δM , G and δG are the mass of star ($1.47 \pm 0.8 M_\odot$), the universal gravitational constant ($6.6741 \pm 0.0003 * 10^{-11} \text{ Nm}^2 \text{ kg}^{-2}$)^[16] and their errors respectively. It should be noted here that the mass of the planet ($3.43 * 10^{27} \text{ kg}$)^[3] which is about 0.0017% the mass of the star and much smaller than error on the star mass, hence can be ignored while using equation (2).

- Dip in secondary intensity was found to be $4.90 \pm 1.04 * 10^{-5}$ with errors determined from equation (15). It is apparent that the error is almost 25% the actual value and can significantly affect the further calculations.

Having found secondary dip intensity, orbital and planetary radius, we computed the geometric albedo to be 0.141 ± 0.069 , which is in agreement with previously found values (≈ 0.13)^[20]. The error was determined using the formula,

$$\delta A_g = A_g * \sqrt{\left(\frac{\delta F}{F}\right)^2 + 2 * \left(\frac{\delta R_p}{R_p}\right)^2 + 2 * \left(\frac{\delta a}{a}\right)^2} \quad (17)$$

where these symbols are defined earlier.

- The phase integral of Kepler 2 was calculated to be 0.22160 ± 0.00002 (no units). This multiplied with albedo gave a value of 0.031 ± 0.007 for bond albedo. Errors in phase integral and bond albedo were calculated from:

$$\delta q = q * \sqrt{\sum_i^n \delta F_i^2 / n} \quad \text{and} \quad (18)$$

$$\delta A_b = A_b * \sqrt{\left(\frac{\delta A_g}{A_g}\right)^2 + \left(\frac{\delta q}{q}\right)^2} \quad \text{respectively.} \quad (19)$$

- Luminosity of the Kepler-2 was determined using equation (6) to be $1.94 \pm 0.57 * 10^{27} \text{ W}$ from the values luminosity of Vega ($40.12 \pm 0.45 L_\odot$)^[17], distance from observer to Kepler-2 ($1100 \pm 160 \text{ ly}$)^[18] and Vega ($25.04 \pm 0.07 \text{ ly}$)^[17]. Errors were estimated from the standard deviation formula.

- We finally calculate the global effective temperature from the data above and we get $2133.91 \pm 127.86 \text{K}$, with errors propagated from the albedo, orbital distance and luminosity.
- Using equations (9),(10) and (11), we found the impact parameter and the inclination angle to be 0.497 ± 0.248 (no units) and 83.5 ± 7.93 deg. The errors were determined by:

$$\delta b = b * \sqrt{\left(\frac{\delta t}{t}\right)^2 + \left(\frac{\delta a}{a}\right)^2 + \left(\frac{\delta R_p}{R_p}\right)^2} \text{ and} \quad (20)$$

$$\delta i = \left[a * \frac{\delta a}{\sqrt{1 - \left(\frac{b}{a}\right)^2}} + \frac{\delta b}{b * \sqrt{1 - \left(\frac{b}{a}\right)^2}} \right] * i. \quad (21)$$

Where a is the normalised orbital distance and t the transit duration. Equation (21) was obtained using the partial derivative approximation to calculate the error.

Table 1: Calculated properties vs accepted values

Kepler-2b properties	OBTAINED VALUES	ACCEPTED VALUES
Period (days)	2.204709	$2.204735471 \pm 0.000002^{[3]}$
Normalised radius	0.0821 ± 0.0145	$0.0763 \pm 0.0011^{[19]}$
Normalised orbital radius	4.407 ± 1.49	$4.35 \pm 0.33^{[19]}$
Impact parameter(in stellar units)	0.497 ± 0.248	$0.37 \pm 0.22^{[19]}$
Orbital inclination (deg)	83.5 ± 7.93	$85.7 \pm 3.3^{[19]}$
Geometric albedo	0.14 ± 0.07	$\approx 0.13^{[20]}$
Bond albedo	0.031 ± 0.007	
Equilibrium temperature(K)	2133.91 ± 127.86	$2140 \pm 85^{[19]}$

- From the physical parameters obtained, we realise that Kepler-2b is a large planet (roughly 1.4 times Jupiter), a short and inclined orbit around a star brighter than our Sun. It has a very low bond albedo (≈ 0.03) which means it reflects about 3% of the incident light, making it a dark and highly irradiated planet. It has also been determined that extremely hot exoplanets ($T > 2100 \text{K}$) have a higher equilibrium temperature than predicted by the blackbody temperature.^[21] It has been found that the temperature can be as high as 2800K on the side facing the star, decreasing the likelihood of condensation, and hence sparse clouds.^[22] This contrast in temperature between the day and nightside could sustain fast winds (due to the planet's short period). Calculating the transit dips over multiple band widths can help constrain the atmospheric composition (since a different composition would absorb and scatter incident light differently based on its wavelength), an objective of this experiment which we couldn't complete. However, research suggests that for hot-Jupiters with $T > 1900 \text{K}$ and low reflectivity, presence of condensate CaTiO_3 , silicate clouds and corundum (Al_2O_3) are most likely.^{[21][22][23]}

Modelling:

- We coded two primary transit models for our data and fitted it using the `curve_fit()` function in python. The errors are returned in a covariant matrix, and errors extracted by taking the root of the diagonal elements.^[9] *Figure 8a* shows our initial 3 parameter model fitted to Kepler-2.

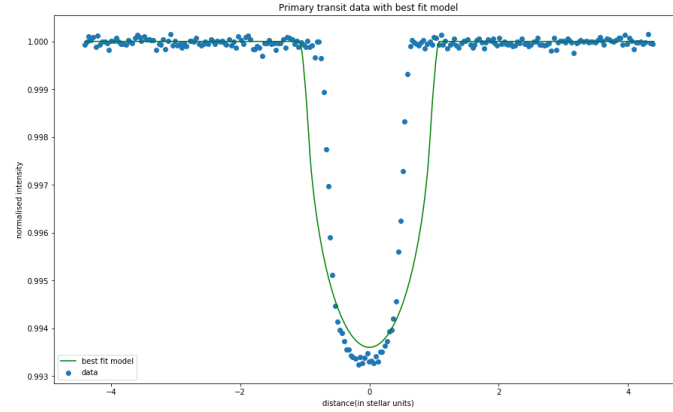


Figure 8: Primary transit model for Kepler-2.

It should be noted that the model was designed to return observed intensities as a function of distance, so we had to convert the times series of our data to a distance scale. This was done by assuming constant tangential velocity v in orbit and the radial velocity as $v \cdot \sin \theta$, $\theta \in [0, \pi]$ and calculating distance. Returned best fit parameters can be found in *Table 2*.

We see that the uncertainties in the best fit parameters are large, and hence needed a better model. *Figure 9* shows a modified 4-parameter model, with the optimal variables in *Table 2*.

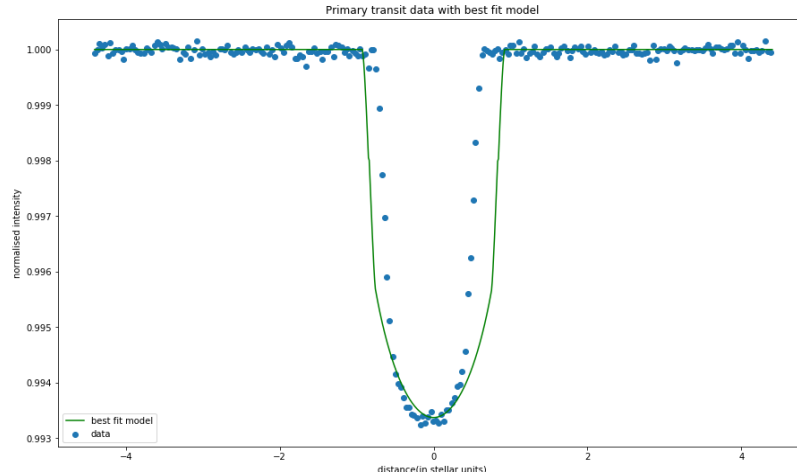


Figure 9: Best fit model with inclination angle.

This model showed significant improvement, which can be seen visually (minimum of the dip is captured, and dip is sharper) and is confirmed when the errors are returned. The residuals were plotted and shown in *Figure 10*.

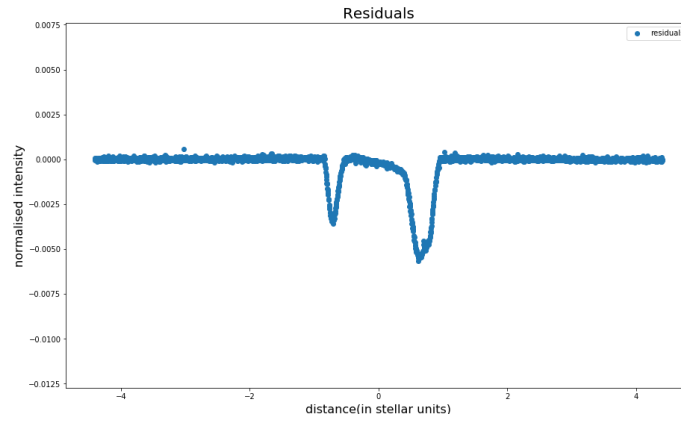


Figure 10: Residual plot for the 4-parameter model with data for Kepler-2.

The residuals suggest that the data wasn't aligned exactly at 0, but an otherwise good fit. Possible improvements in the model could be done by including limb-darkening effects for the intensity. We could also search for correlations in the residuals to find misspecifications in our model but wasn't attempted due to time constraints.

Table 2: Optimal parameters with errors

Parameters	3-parameter model	4-parameter model
Normalised planet radius	$0.082 \pm 1.96 \cdot 10^3$	$0.083 \pm 9.32 \cdot 10^{-6}$
Star radius	$0.995 \pm 2.54 \cdot 10^4$	0.995 ± 0.01
Star intensity	$1.0 \pm 7.2 \cdot 10^{-5}$	$1.0 \pm 6.3 \cdot 10^{-5}$
Impact parameter		0.54 ± 0

- Coded a secondary transit model, which used best fit values from the model above in addition to planet intensity and albedo. Bounds were set based on the errors in *Table 1* and the result is shown in *Figure 11*. The large errors suggested that this model wasn't accurate to extract albedos for smaller exoplanets.

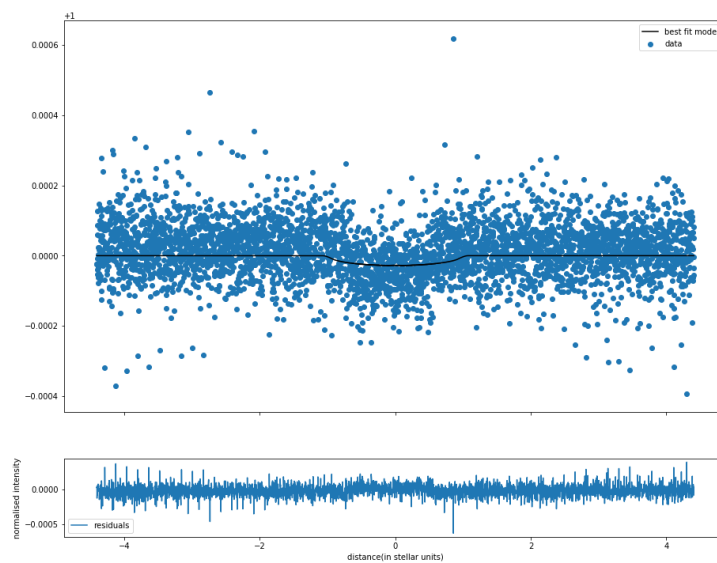


Figure 11: Secondary transit model with data. Data shown here was binned (bin-size=10) to reduce computation time. Returned value for albedo $A_g = 0.59 \pm 463.8$.

Conclusion:

The main objective of the project was to determine the weather on a hot Jupiter using albedo and the other physical parameters. This was achieved with significant accuracy for Kepler-2, and the most likely atmospheric composition proposed. We also presented a thorough error analysis for all the values obtained except period. Custom primary and secondary models were designed and fitted, and the results tabulated. However, we could improve on our results by:

- Analysing the transit over the infrared spectrum from *Spitzer*, to obtain a more robust idea of the winds in the atmosphere.^[23]
- Introduction of limb-darkening coefficients in the primary transit model and a good secondary transit model to obtain accurate values for albedo.
- Repeating the experiment for other Hot-Jupiters, to compare with Kepler-2.

Studying atmospheres of exoplanets remains a relatively new field, and improved resolution of the emission spectrum from exoplanets should help constrain the atmospheric compositions significantly.

Acknowledgements:

We are extremely grateful for the support provided by our lab demonstrator Ben Rendle as well as the lab leader Dr. Graham P. Smith. I would also like to thank my group members Alice Purdy and Sharif Khan-Bennett for helping achieve the goals of the experiment. Finally, the research required lightcurves which was gathered from NASA's mast archive, exoplanet.eu for candidates and the lightkurve tutorials for processing.

References:

- [1] MAST Database, <https://archive.stsci.edu/kepler/lightcurves.html> (accessed 2019)
- [2] NASA Exoplanet archive, https://exoplanetarchive.ipac.caltech.edu/docs/counts_detail.html (accessed 2019)
- [3] Kepler-2b, http://exoplanet.eu/catalog/hat-p-7_b/ (accessed 2019)
- [4] Wilson, Paul A. <https://www.paulanthonywilson.com/exoplanets/exoplanet-detection-techniques/the-exoplanet-transit-method/> (accessed 2019)
- [5] https://www.researchgate.net/figure/Optical-phase-curve-of-the-planet-HAT-P-7bobserved-by-Kepler-26-showing-primary_fig4_51963834 (accessed 2019)
- [6] Showman, Adam P. et al. <https://arxiv.org/abs/0911.3170> (2009)
- [7] Jacob, Daniel J. <http://acmg.seas.harvard.edu/people/faculty/djj/book/bookchap7.html> (accessed Feb 2019)
- [8] Latham, David, W. et al. <https://iopscience.iop.org/article/10.1088/2041-8205/713/2/L140/> (2010)
- [9] Kepler-7b, http://exoplanet.eu/catalog/kepler-7_b/ (accessed 2019)
- [10] Lightkurve, <https://docs.lightkurve.org/tutorials/index.html> (accessed 2019)
- [11] Kepler Science centre, <https://keplergo.arc.nasa.gov/PyKEprimerLCs.shtml> (accessed 2019)

- [12] SciPy, <https://www.scipy.org/docs.html> (accessed 2019)
- [13] Chaplin, W. <https://canvas.bham.ac.uk/courses/34223/files/6029916/download?wrap=1> (accessed 2019)
- [14] Kepler-78b http://exoplanet.eu/catalog/kepler-78_b/ (accessed 2019)
- [15] Mandel, K. & Agol, E. <https://iopscience.iop.org/article/10.1086/345520> (2002)
- [16] The NIST Reference, <https://physics.nist.gov/cgi-bin/cuu/Value?bg> (accessed 2019)
- [17] Vega, <https://en.wikipedia.org/wiki/Vega> (accessed 2019)
- [18] HAT-P-7, <https://en.wikipedia.org/wiki/HAT-P-7> (accessed 2019)
- [19] Pal, A. et al. <https://iopscience.iop.org/article/10.1086/588010/pdf> (2008)
- [20] Christiansen, J. et al. <https://iopscience.iop.org/article/10.1088/0004-637X/710/1/97/pdf> (2009)
- [21] Parmentier, V. et al. <https://ui.adsabs.harvard.edu/#abs/2016ApJ...828...22P> (2016)
- [22] Armstrong, D. J. et al. <https://www.nature.com/articles/s41550-016-0004> (2016)
- [23] Garhart, E. et al. <https://arxiv.org/abs/1901.07040> (2019)